Terahertz Absorption of DNA Decamer Duplex

Xiaowei Li,[†] Tatiana Globus,[*,†] Boris Gelmont,[†] Luiz C. Salay,[‡] and Alexei Bykhovski[†]

Department of Electrical and Computer Engineering, University of Virginia, Charlottesville, Virginia 22904, and Department of Molecular Physiology and Biological Physics, University of Virginia, Charlottesville, Virginia 22908

Received: July 25, 2008

This work combines experimental and theoretical approaches to investigate terahertz absorption spectra of the DNA formed by the sequence oligomer 5′-CCGGCGCCGG-3′. The three-dimensional structure of this self-complimentary DNA decamer has been well-studied, permitting us to perform direct identification of the low-frequency phonon modes associated with specific conformation and to conduct comprehensive computer simulations. Two modeling techniques, normal-mode analysis and nanosecond molecular dynamics with explicit solvent molecules, were employed to extract the low-frequency vibrational modes based on which the absorption spectra were calculated. The absorption spectra of the DNA decamer in aqueous solution were measured in the frequency range 10−25 cm^{-1} using the terahertz Fourier transform infrared spectroscopy. Multiple well-resolved and reproducible resonance modes were observed. When calculated and experimental spectra were compared, the spectrum based on molecular dynamics simulations showed a better correlation with the experimental spectra than the one based on normal-mode analysis. These results demonstrate that there exist a considerable number of active low-frequency phonon modes in this short DNA duplex.

Introduction

There is considerable interest in investigating absorption features of biological molecules (DNA and proteins) in the terahertz (THz) or submillimeter wave range, 0.1−10 THz (or 3−300 cm^{-1}) both experimentally and theoretically.[1−8] The spectral features in the THz frequency range primarily originate from poorly localized, collective motions of biomolecules. Such collective motions play important roles in the function processes of these macromolecules (for example, in transcribing genetic information from DNA to RNA[9]). Furthermore, these low-frequency vibrational modes are sensitive, as the theoretical calculations have predicted, to the sequences and molecular conformations. Therefore, measurements of low-frequency vibrational motions eventually should disclose information regarding the three-dimensional structure and flexibility of polymers. The THz spectral features of the biological materials may serve as the characteristic fingerprints leading to the potential applications of terahertz spectroscopy in biomedical sciences.[6]

This work focuses on the experimental and theoretical investigation of the THz absorption features of a well-known self-cDNA oligomer 5′-CCGGCGCCGG-3′. The molecular structure and helical conformation of this DNA decamer has been well-characterized using X-ray[10] and circular dichroism (CD) spectroscopy,[11] which allows us to seek the direct relationship between THz phonon modes and the molecular conformation. These earlier studies demonstrated that the DNA decamer adopts the canonical B-form helical structure in aqueous solution and it can be converted to the A-form structure by dehydration. Our measured circular dichroism spectrum of the decamer suggests that the molecule can potentially form intercalated tetraplex structure upon dehydration using trifluorethanol in acidic environment. The transmission spectra of the aqueous-phase DNA decamer in the frequency range 10−25 cm^{-1} were measured using the terahertz Fourier transform infrared (FTIR) spectroscopy. In parallel with the experimental study, the computer modeling and simulation of the B-form DNA decamer were performed using normal-mode analysis and molecular dynamics (MD) and the THz absorption spectra were calculated. Both calculated spectra were compared with the measured spectra to evaluate performance of the two molecular modeling techniques to predict THz absorption features of biological molecules.

Experimental Methods

The oligonucleotides were purchased from Integrated DNA Technologies, Inc. The lyophilized DNA fragments were dissolved in 50 mM NaCl water. The pH of the solution is within the range 5.3−5.9. Annealing technique was applied to ensure that DNA can adopt standard and stable double-helix form since the purchased DNA molecules were single-stranded. In the annealing process, the DNA solution was heated to 94 °C, kept for 2 min in water bath, and then cooled to room temperature gradually. Circular dichroism spectroscopy[12,13] was employed to confirm the secondary structure of the DNA molecules after annealing. The CD spectrum of the decamer was measured using the AVIV model 215 circular dichroism spectrometer (AVIV Biomedical, Inc.) in 0.05-cm path length Hellma cell placed in a thermostatted holder. All CD measurements were taken at 22 °C. The frequency of the CD spectra covers a 320−200-nm range. Note that the ellipticity is reported in units of M^{-1} cm^{-1} in which the molar unit, M, is related to the nucleoside residues of DNA for comparison with an earlier result.[11]

The THz transmission spectra measurement started from sample preparation. The DNA solution was diluted to 0.1−3 mg/mL. The samples were prepared by sandwiching an appropriate amount (∼10−20 μL) of DNA solution between two very thin (∼10 μm) and THz radiation transparent (∼97−99%)

* To whom correspondence should be addressed. Phone: 434-924-7709. Fax: 434-924-8818. E-mail: tg9a@virginia.edu.
† Department of Electrical and Computer Engineering.
‡ Department of Molecular Physiology and Biological Physics.

10.1021/jp806630w CCC: $40.75
Published on Web 10/18/2008

TABLE 1: DNA Decamer (5′-CCGGCGCCGG-3′) Samples Measured in This Work

sample no.	concentration (mg/mL)	substrate
BB1916	0.1	SF[a]
BB1930	0.1	SF
BB2560	0.3	SF
BB2561	0.3	SF
BB1918	1	SF
BB2002	1	SF
BB1977	3	SF
BB2541	3	SF
BB2021	3	PC[b]

[a] SF = Saran film. [b] PC = polycarbonate.

films, polyethylene (PE) and polycarbonate (PC). The PE film we used in the experiment was Saran film (SF) manufactured by S. C. Johnson Corp. The thickness of the sample was adjusted by Teflon rings with an inner diameter of 18 mm and thickness in the range 12−75 μm. At least two samples of each concentration were measured to obtain reliable THz spectra of dilute DNA solution in the 10−25 cm^{-1} range. For each sample, several measurements were repeated to ensure the reproducibility of spectral features, especially the frequencies of resonance peaks. The information (sample number, concentration, and substrate material) of measured samples is summarized in Table 1.

The THz transmission spectra of DNA materials were measured and recorded using the IFS-66v FTIR spectrometer manufactured by Bruker Instruments. The earlier test measurements using a wire polarizer indicated 80% polarization of radiation in FTIR spectrometer in the spectral range of interest and the electric field vector E oriented preferably in the vertical direction. A Si-bolometer was operated at the liquid helium-cooled temperature (1.7 K) for signal detection. Spectral resolution in this study was 0.25 cm^{-1}, which was dictated by the characteristic dissipation parameter or the spectral width of low-frequency vibrational modes (∼0.5 cm^{-1} [14]). A Mylar beamsplitter of 125-μm thickness was used for the measurements in the spectral range 10−25 cm^{-1}. The optical aperture was set to 12 mm, and the scan velocity was 80 kHz. In addition, a cooled filter with a cutoff frequency of 35 cm^{-1} was used inside the bolometer cryostat. Other parameters and software settings included a phase resolution of 2 cm^{-1}, the acquisition function "single-sided, fast return", zero filling factor of 4, and the "Blackman-Harris three-term" apodization function. To reduce the noise level, every measurement involved an average of 32 scans. Under these settings, the signal-to-noise ratio was >500 and the reproducibility of the instrument in transmission mode was better than 0.2−0.3% in almost the entire spectral range, although it became worse at both ends because of the rapid reducing of radiation intensity (Figure 1). Additional details of the experimental technique can be found in ref 15.

The sample was placed in a standard Bruker sample holder in the focus of the beam inside the sample compartment. The whole instrument, except for the sample compartment, was evacuated to 10 mbar. Two steps were taken in measuring the transmission, T, of the DNA sample. First, the spectrum of a sample holder having an aperture smaller than the internal diameter of the sample assembly was recorded as the background or reference spectrum. Second, a sample spectrum was measured and divided by the background spectrum to obtain the transmission T. Resonance features in the transmission spectra of water layers between thin films were demonstrated

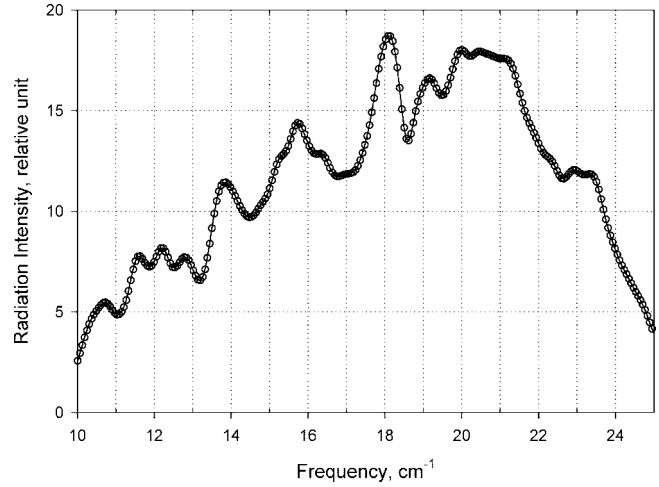

Figure 1. Intensity of radiation passing by the DNA sample in a Bruker IFS-66v spectrometer.

in this sub-THz range. Among these absorption features, only one structure at 18.6 cm^{-1} was caused by disturbances from water vapor in air in our spectral range. All other features resulted from absorption by liquid water and substrate material. To extract the absorption features of biological material from others (water and substrate material), we recalculated each transmission spectrum of DNA solution against the transmission spectrum of pure water put in a similar sandwich cell. Specifically, the transmission spectrum of the DNA molecule was obtained by dividing the spectrum of the DNA solution using the spectrum of water with the same or slightly higher level of transmission. One drawback associated with this approach is that the resulted transmission intensity cannot represent the absolute transmission level of DNA material. It is almost not possible to exactly match the transmission levels of water to that of the DNA solution. However, we found that the positions of transmission minima (or the absorption maxima in the corresponding absorption spectrum) on the frequency scale in the recalculated transmission spectrum were not shifted or changed by the different selections of the water transmission spectra, which is consistent with previous demonstrations.[15,16] Thus, our approach gives rather accurately the absorption peak positions on the frequency scale and the relative intensities of different absorption peaks.

Molecular Modeling

Energy Minimization and Normal-Mode Analysis of the DNA Decamer. The starting point of the normal-mode analysis of the DNA decamer molecule was to build the B-form DNA molecule with sequence 5′-CCGGCGCCGG-3′ using the structure parameters from X-ray diffraction of DNA fiber. The structure parameters are included as library files in the AMBER 8 package.[17] Eighteen sodium ions, in terms of the number of phosphate groups, were added to neutralize the DNA fragment using the ADDIONS routine implemented in AMBER. The ADDIONS routine works by constructing a Coulombic potential on a 1.0 Å grid and then placing sodium ions at the points of the lowest electrostatic potential. After the molecule was built, the total potential energy was calculated as the sum of covalent bond energy, covalent angle energy, proper and improper torsions, nonbonded interactions including electrostatic, and van der Waals interactions using the AMBER 99 force field.[18] The potential energy was then minimized using conjugate gradient or Newton−Raphson minimization techniques in the Cartesian

coordinate space as in ref 19. The convergence criterion of the energy minimization was that the root-mean-square of the energy gradient was less than 10^{-4} kcal/mol·Å. To take into consideration the solvent effect on the simulation, the distance dependence dielectric constant ($\varepsilon_r = r$) was used. Although it is not a rather physically realistic model for the solvent effect on the system energy, the distance dependence dielectric constant method has produced a reasonable well approximation of solvent effect as previous simulation work has demonstrated.[20] The normal-mode analysis was performed using the NMODE module in the AMBER 8 suite. The resulting vibrational frequencies and eigenvectors were used to calculate the absorption spectrum of corresponding molecules in the terahertz region using the computational method proposed in ref 21.

Molecular Dynamics Simulation of the DNA Decamer. Our molecular dynamics simulations of the DNA decamer, 5′-CCGGCGCCGG-3′, were performed using the SANDER module of the AMBER 8 suite, and the detailed preparation procedure of the simulation was similar to that in ref 22. The initial process to produce the neutralized DNA molecular complex was the same as that used for normal-mode analysis. After this, the DNA−ion complex was solvated in a cubic water box (i.e., TIP3P water molecules) with the dimension of ~63 Å in each side, allowing at least 12 Å water shell around DNA. The solvent box contains ~7400 water molecules. Initial energy minimization was performed on the solvent molecules and ions while the DNA was kept fixed with the harmonic restraint of 500 kcal/mol/Å^2. Following the energy minimization of the whole system including DNA, water, and counterions, the molecular system was slowly heated to 300 K from 0 K at constant volume in 100 ps while the DNA was restrained by the penalty energy of 25 kcal/mol/Å^2. To slowly release these restraints, we conducted a series of five segments of 1000 steps of energy minimization and 50-ps equilibration with constant temperature (300 K) and constant pressure (1 bar) via the Berendsen algorithm[23] with a coupling constant of 0.2 ps for both parameters as Beveridge et al. used.[22] The final stage of equilibration consists of a 50-ps simulation with a restraint of 0.5 kcal/mol/Å^2 and 50-ps unrestrained simulation. The production simulation with constant volume and constant temperature (NVT) ensemble started after the equilibration. Electrostatic interactions were treated using the particle mesh Ewald algorithm[24] with a real space cutoff of 10 Å, cubic B-spline interpolation onto the charge grid with a spacing of approximately 1 Å. A weak coupling algorithm with a coupling constant of 5 ps was used to stabilize the temperature. The first 50-ps simulation in the NVT ensemble was used for further equilibration of the system and therefore was not included in the later analysis of the trajectory. The integration time step was 1 fs and the molecular trajectory was saved every 0.1 ps. The total simulation length was 10 ns.

Quasi-Harmonic Analysis of the Molecular Trajectory. Quasi-harmonic analysis (QHA), also called essential dynamics or principle component analysis, was initially developed by Karplus et al. for the calculation of the thermodynamic properties of molecules with trajectories from molecular dynamics simulation.[25,26] The essential idea behind the QHA is that the Hamiltonian of the system can be parametrized to a general and effective quadratic function while the coefficients in the quadratic terms can be chosen in accordance with the calculated fluctuations from the simulation results of molecular dynamics on the complete multidimensional potential energy surface. As the first step of quasi-harmonic analysis, the trajectories of DNA molecule were extracted from the solution trajectories by stripping water and counterion trajectories. Then, DNA trajectories were aligned against a reference structure (i.e., the initial ideal B-form DNA conformation) to remove global translational and rotational differences between snapshots, which was implemented using the rms command of ptraj, the analysis program of AMBER suite. The mass-weighted covariance matrix, which describes the correlations between atomic positional fluctuations in the DNA, was then built after the fitting procedure as:

$$\sigma_{ij} = M_i^{1/2}\langle [x_i(t) - \langle x_i \rangle][x_j(t) - \langle x_j \rangle] \rangle M_j^{1/2} \quad (1)$$

where σ is the mass-weighted covariance matrix, M is the mass of atoms, $x_i(t)$ and $x_j(t)$ are the atomic coordinates of the i-th and j-th atoms at time t, while $\langle\ \rangle$ denotes averaging over the time period of simulation. In the quasi-harmonic approximation framework, the force constant matrix is related to the covariance matrix as in:[26]

$$F = k_B T \sigma^{-1} \quad (2)$$

where F is the force constant matrix, k_B is the Boltzmann constant, and T is the temperature. The diagonalization of the force matrix F yields the vibrational frequencies and the corresponding amplitudes based on which the absorption spectrum of the decamer was calculated using the computational method presented early in ref 21.

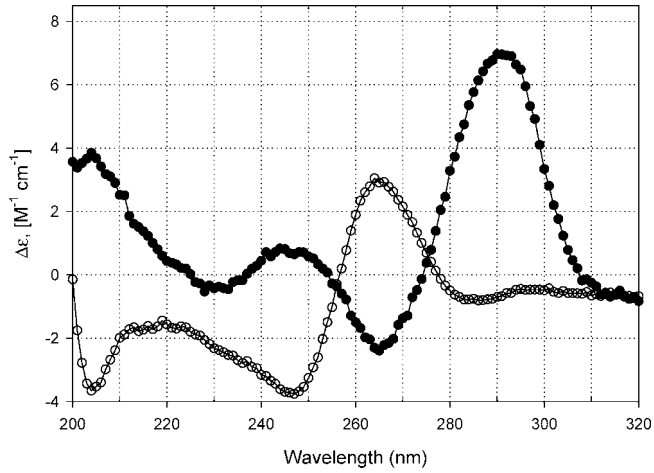

Figure 2. Circular dichroism spectra of the self-cDNA decamer 5′-CCGGCGCCGG-3′ in two different buffers promoting B (○) and a tetraplex form (●): 50 mM NaCl, pH = 5.3, and 18% (w/w) 2.5 mM NaCl, 1 mM NaH_2PO_4, 0.1 mM EDTA, pH = 5.9, plus 82% (w/w) TFE.

Results and Discussion

Experimental Results. Figure 2 shows the CD spectra of the DNA decamer in two different buffers: 50 mM NaCl, pH = 5.3, and 18% 2.5 mM NaCl, 1 mM NaH_2PO_4, 0.1 mM EDTA, pH = 5.9, plus 82% (w/w) trifluorethanol (TFE). The CD spectrum of DNA in 50 mM saline exhibits the typical CD spectral features of B-form DNA (i.e., a positive band at 260−270 nm and two negative bands of similar magnitudes at 200−210 and 240−250 nm). These features agree well with the previously reported results of the same B-form DNA decamer in ref 11. On the other hand, we did not observe the characteristic CD spectral features of A-form DNA (i.e., deep negative band around 210 nm, a negative shoulder in the vicinity of 230 nm, and the strong positive band between 260 and 270 nm) by adding 60% (w/w) ethanol or 82% (w/w) TFE into the

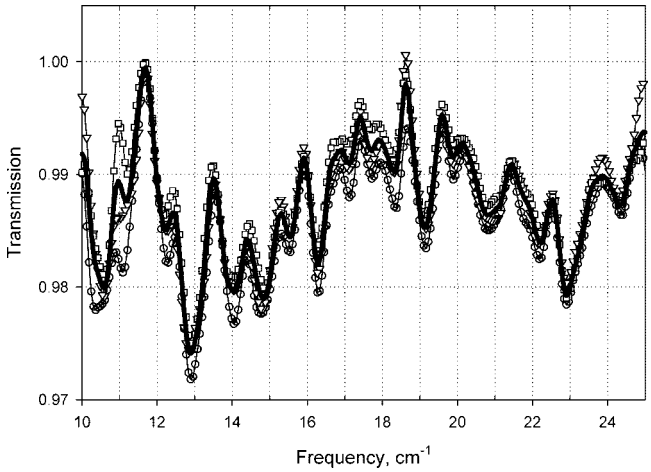

Figure 3. THz transmission spectra of a DNA decamer sample (BB2560, 0.3 mg/mL, Saran film substrate). Two transmission spectra (▽ and ○) were obtained using the same reference spectrum, whereas a new reference spectrum was used for the third transmission spectrum (□). The smooth thick curve without symbols is the average of the three spectra.

B-form DNA solution, indicating the DNA did not adopt the A form under these conditions. However, the DNA decamer in 82% TFE at acidic pH produces an CD spectrum with a strong positive peak at 290 nm and a broad negative band between 260−270 nm and a small negative band at 230 nm. These features are characteristic for an acid-induced intercalated tetraplex of DNA as observed, for example, with the oligomer d(TCCCCACCTTCCCCACCCTCCCCACCCTCCCCA)[27] under our experimental conditions. This assignment is only tentative and deserves deeper investigation. The reason why we did not observe a transition from the B to A form is not cleary at this moment.

For each prepared sample, the measurements of absorption spectrum were repeated several times to ensure that the measured spectral features (particularly the transmission minima) were reproducible. Figure 3 shows the transmission spectra in the 10−25 cm^{-1} range of B-form DNA at 0.3 mg/mL (sample BB2560, SF substrate) obtained from three measurements. The first two spectra were measured successively sharing the same background or reference spectrum, whereas a new background spectrum was recorded with the third transmission spectrum. The three measurements yielded very similar results, which demonstrates the reliability and reproducibility of our experimental setup.

The orientation dependence of spectral features, which was reported in an early study of long DNA polymers,[15,16] was also observed during our experiment. Figure 4 compares the absorption spectra of the same sample (BB1916) oriented in two different directions, 0 and 90°. Note that the relative angles mentioned here refer to the sample rotation by 90° on the holder to ensure all samples have the same preparation and measurement procedures. This rotation reflects changing of the sample relative to the electric field direction in our vertically polarized THz beam. Significant differences were observed between these two transmission spectra. For example, a pronounced transmission minimum at 14 cm^{-1} was present in the spectrum of 90° orientation, whereas the spectrum of 0° orientation produced a transmission maximum at 14 cm^{-1}. The orientation dependence effect indicates that the DNA molecules were somehow oriented in the measured samples. The orientation of the DNA molecules in a thin layer is quite possibly caused by the interactions between the molecule and the substrate material. However, we

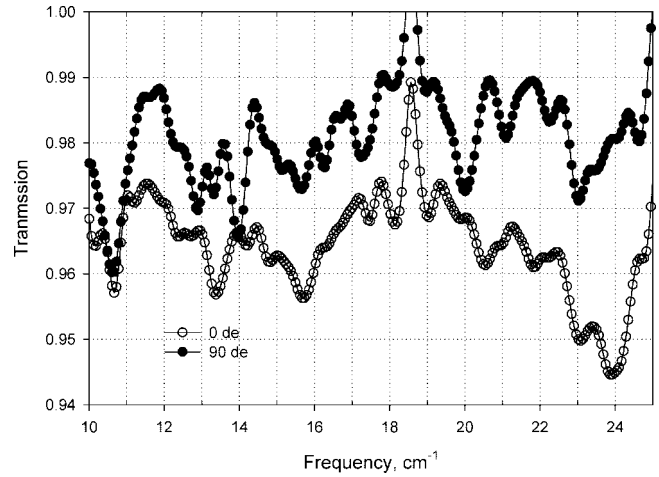

Figure 4. Measured transmission spectra of sample BB1916, in two orientations, 0 and 90°.

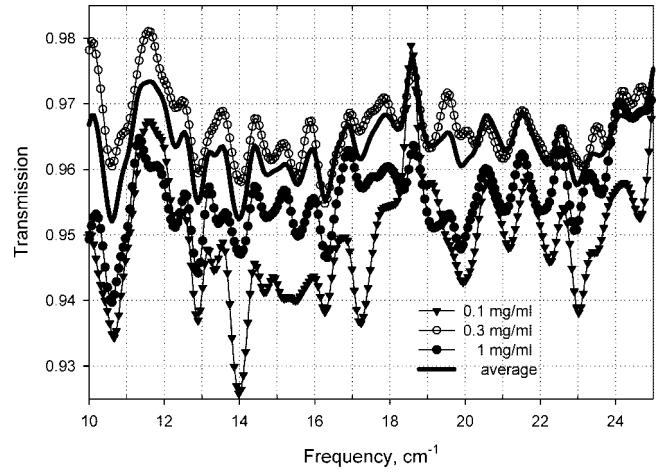

Figure 5. Transmission spectra of DNA decamer samples with different concentrations (0.1, 0.3, and 1 mg/mL) and the average.

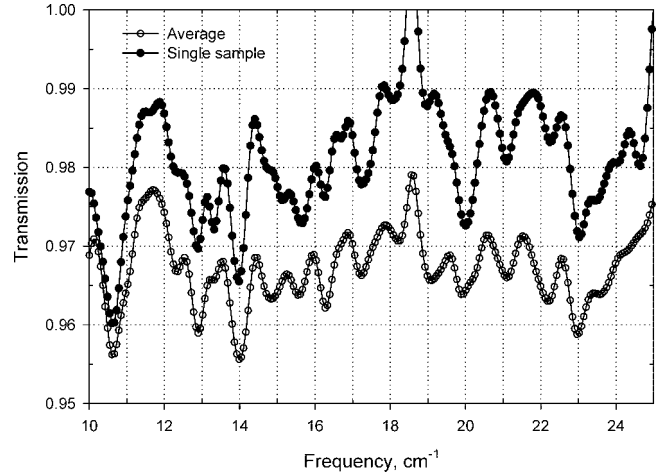

Figure 6. Comparison of average transmission spectra of all samples with the transmission spectrum of one single sample of 90° polarization (BB1916).

also observed that there were no strong orientation effects in many measured samples, suggesting that the alignment of short DNA molecules was easily destroyed. In other words, the measured spectra included the contributions of DNA decamer oriented in different directions relative to the electrical field of radiation. Therefore, we compared the measured spectra only with the average of calculated spectra in three orientations (one

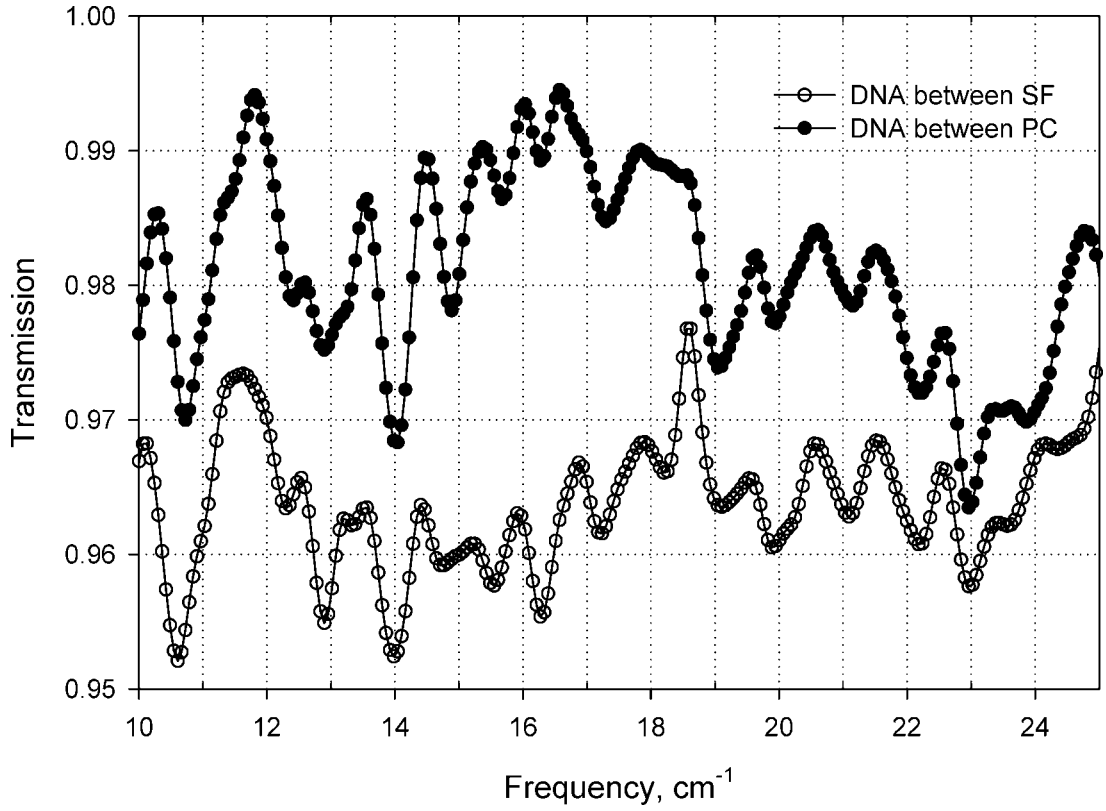

Figure 7. Transmission spectra of DNA decamer between Saran film and polycarbonate (sample BB2021) substrates.

parallel to the helical direction and two perpendicular). The dependence of spectral features on sample orientation makes it rather difficult for us to compare spectra from different samples and to confirm the reproducibility of spectral features. However, we found that the resonance peak at 14 cm^{-1} is particularly sensitive to the sample orientation and can serve as the indicator of sample orientation, which is also reported in earlier studies.[14−16] Therefore, we only selected the spectra with a minimum at 14 cm^{-1} in our analysis.

As an important step to confirm the reliability and reproducibility of the observed resonance modes, we compared the transmission spectra of DNA decamer with different concentrations and substrate materials. The spectra of samples with concentrations of 0.1, 0.3, and 1 mg/mL are shown in Figure 5. It can be seen from Figure 5 that the positions of almost all pronounced peaks (for example, 10.5, 12.9, 14, and 16.3 cm^{-1}) are reproduced quite well despite the concentration variations. At the same time, the intensities of these reproduced peaks can be different. The intensity differences are most likely related to the orientation-dependence effect. Because of the variation of peak intensity, the peaks in the average spectrum of all concentrations usually are less pronounced than the peaks in an individual sample spectrum, which is evidenced in Figure 6. The influence of the substrate material on the absorption features was investigated by comparing the transmission spectra of samples using SF and PC substrates. In Figure 7, the average transmission spectrum of samples using SF substrate was compared with the transmission spectrum of the sample (BB2021) using PC substrate. The absorption peaks agree well with each other, showing that the average resonance peaks are independent of substrate materials. These experimental results demonstrate that there exist a considerable number of active low-frequency vibrational modes associated with short DNA molecule in the terahertz region. Furthermore, these low-frequency modes can be observed even for the DNA solution

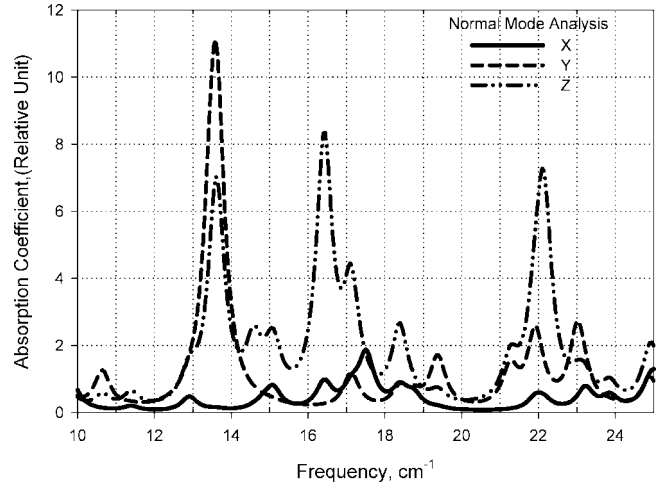

Figure 8. Calculated absorption spectra (10−25 cm^{-1}) of DNA decamer in three polarization directions *X* (solid line), *Y* (dash line), and *Z* (dash−dot−dot line) based on the normal-mode (NM) analysis.

with very low concentration using the terahertz Fourier transform spectroscopic technique. In all cases, we eliminated features at 18.6 cm^{-1} since it was caused by mismatch between water vapor in ambient air during the sample and reference measurements.

Modeling Results. Figures 8 and 9 show the calculated absorption spectra of the DNA decamer in three polarization directions (*X*, *Y*, and *Z*) based on the normal-mode analysis and molecular dynamics. The *Z* direction is parallel to the helix direction, whereas the *X* and *Y* directions are perpendicular to the helix direction. A considerable number of distinguished absorption peaks was present in both results. At the same time, each direction demonstrated unique spectral features (i.e.,

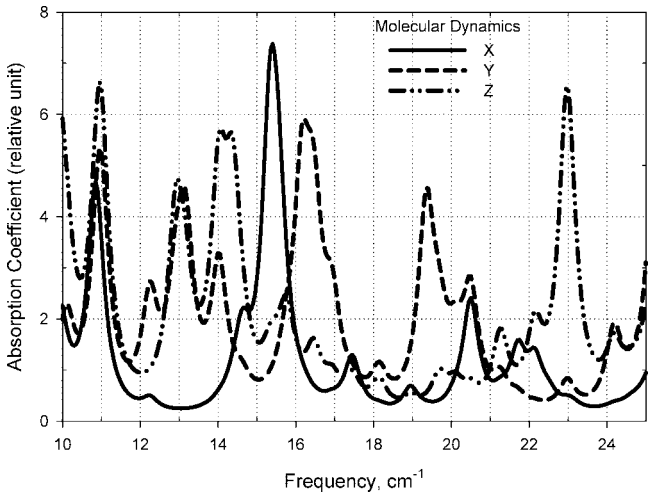

Figure 9. Calculated absorption spectra (10−25 cm^{-1}) of DNA decamer in three polarization directions *X* (solid line), *Y* (dash line), and *Z* (dash−dot−dot) based on the 10-ns explicit solvent MD simulation.

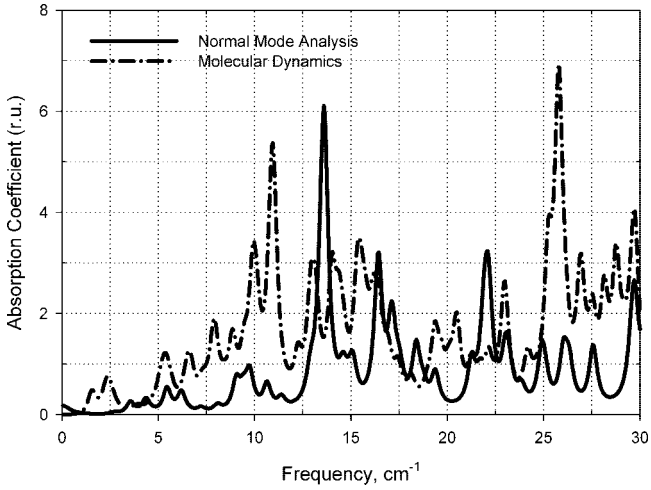

Figure 10. Comparison of the average absorption spectra (0−30 cm^{-1}) based on normal-mode analysis and molecular dynamics simulation.

resonance peaks and intensities), which explains the orientation dependence effect observed in this experiment.

In Figure 10, we compare the calculated transmission spectra in the frequency range 0−30 cm^{-1} based on two computing techniques. Note that the absorption spectra in this figure are average spectra of three polarization directions. Common spectral features are shared between these two calculated spectra. For example, several distinguished peaks, 16.3, 19.3, 22, 23 cm^{-1}, are present in both spectra. In addition, both computing techniques predicted that the absorption peaks below 10 cm^{-1} are less pronounced than the peaks above 10 cm^{-1}. However, significant differences are observed between these two spectra. In the frequency below 10 cm^{-1}, the molecular dynamics simulation produced several distinguished (relative intensity more than 1) absorption peaks, whereas the normal-mode analysis did not yield any peak with relative intensity more than 1. The normal-mode analysis predicts a strong absorption peak at 13.6 cm^{-1} which is not present in the spectrum of molecular dynamics. These spectral differences most likely root from anharmonicity associated with the low-frequency motions which are discussed below.

Comparison between Theoretical and Experimental Results. Figure 11 compares the calculated absorption spectra with the experimentally measured spectrum of the decamer in the

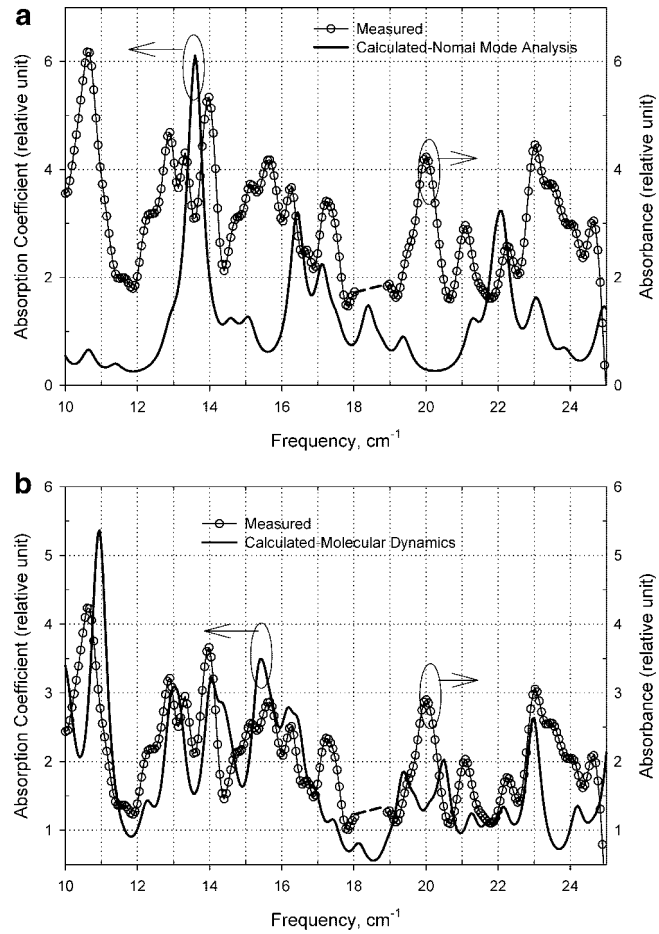

Figure 11. (a) Comparison between the measured absorption spectrum and calculated spectra of the DNA decamer based on normal-mode analysis. (b) Comparison between the measured absorption spectrum and calculated spectrum of the DNA decamer based on 10-ns explicit solvent molecular dynamics simulation.

frequency range 10−25 cm^{-1}, and the absorption peaks are listed in Table 2 for comparison. The experimental result is absorbance spectra of sample BB1916 oriented at 90°. The absorption features in the 18−19 cm^{-1} range were removed because water vapor produced a relatively strong absorption peak at 18.6 cm^{-1}. Although the orientation effect was observed in the measurement, the orientations of the DNA molecules in the liquid phase cannot be well controlled in the current experiment. As mentioned in the Experimental Methods, it is most likely that each direction contributes features to the measured spectrum. Therefore, the calculated three directions' spectra were averaged to compare with the measured absorption spectrum. As shown in Figure 11a,b, both theoretical modeling techniques reproduced fairly well many measured absorption features (for instance, 10.6, 16.3, 17.2, 21.1, 22.2, 23 cm^{-1} peaks) although differences are still observed between theoretical and experimental results. Most important, both theoretical results produced relatively strong absorption peaks around 14 cm^{-1}, which is one of the most distinguished peaks observed here and elsewhere. However, the strong peak at 13.6 cm^{-1} of the NM result has a 0.4 cm^{-1} shift from the measured 14 cm^{-1} peak, while the MD result reproduced well the resonance frequency of this distinguished peak. In the frequency range 10−17 cm^{-1}, it can be easily seen that the MD simulation reproduced the positions of absorption peaks better than the normal-mode analysis. The normal-mode analysis, on the other hand, did predict the

TABLE 2: Measured and Calculated Absorption Peaks Associated with the DNA Decamer (Unit: cm^{-1})

experimental	normal mode analysis	molecular dynamics
10.6	10.6	10.9
11.5 (w[a])	11.4 (w)	
12.3 (s[b])		12.3 (w)
12.9		13
13.3	13.6	
14		14
14.8 (s)	14.6 (w)	14.4 (s)
15.1 (w)	15.1 (w)	
15.6		15.4
16.3	16.4	16.2
16.8 (w)		16.9 (s)
17.2	17.1	17.4 (w)
	18.4	18.1
	19.4	19.4
20		20.5
21.1	21.3 (w)	21.2/21.7 (w)
22.2	22	22.1
23	23	23
23.5 (s)	23.8 (w)	
24 (s)		24.2
24.7	25	25

[a] w = weak. [b] s = shoulder.

absorption peaks reasonably well in the frequency range higher than 16 cm^{-1}.

A couple of factors can contribute to the different predictions of the THz absorption spectra by the normal-mode analysis and molecular dynamics. It is well-known that the normal-mode analysis requires the harmonic approximation of the potential energy. An earlier study showed that the anharmonicity has to be considered for modes below 80 cm^{-1}.[28] The recent investigation of the solvent effect on low-frequency collective motions of DNA demonstrated that low-frequency DNA dynamics is affected by the interactions with the solvent in hydration shell.[29] The molecular dynamics simulation in full potential energy can account for the anharmonicity associated with the low-frequency motions. Therefore, the molecular dynamics simulation can predict the slow motions of biological molecule better than the normal-mode analysis.

Conclusions

This work reports the THz absorption spectra of the DNA decamer with the sequence 5′-CCGGCGCCGG-3′ in aqueous phase measured by terahertz Fourier transform spectroscopy. The experimental results demonstrated that multiactive resonance modes associated with the DNA decamer exist in the THz and submillimeter frequency regions. It is also shown that these resonance peaks can be reproducibly obtained through the measurements of considerably diluted DNA decamer solution. In addition, we compared the ability of the normal-mode analysis and nanoseconds molecular dynamics simulation in explicit water to predict the THz absorption features of DNA molecules. A nanosecond molecular dynamics simulation in explicit solvent predicts the experimentally observed absorption peak positions better than normal-mode analysis in terms of resonance frequencies. It potentially permits better understanding of the nature of low-frequency vibrational modes and the link to the three-dimensional structure of biological molecules.

Acknowledgment. This work was supported by the UVA grant from the W. M. Keck Foundation and in part by U.S. Army NGIC Contract No. DASC01-01-C0009. We thank Dr. Lukas K. Tamm, Department of Molecular Physiology and Biological Physics, University of Virginia, for significantly contributing, guiding, and helping us during the whole work. We are grateful to Dr. Michaela Vorlíčková, Institute of Biophysics, Academy of Sciences of Czech Republic, for her helpful instruction on circular dichroism spectroscopy.

Supporting Information Available: This material is available free of charge via the Internet at http://pubs.acs.org.

References and Notes

(1) Woolard, D. L.; Brown, E. R.; Pepper, M.; Kemp, M. *Proc. IEEE* **2005**, *93*, 1722–1743.
(2) Tonouchi, M. *Nat. Photonics* **2007**, *1*, 97–105.
(3) Laman, N.; Sree Harsha, S.; Grischkowsky, D. *Biophys. J.* **2007**, *107*, 113647.
(4) Shen, S. C.; Santo, L.; Genzel, L. *Int. J. Infrared Millimeter Waves* **2007**, *28*, 595–610.
(5) Liu, H.-B.; Zhong, H.; Karpowicz, N.; Chen, Y.; Zhang, X.-C. *Proc. IEEE* **2007**, *95*, 1514–1527.
(6) Siegel, H. P. *IEEE MTT-S Int. Microwave Symp. Dig.* **2004**, *3*, 1575–1578.
(7) Globus, T. R.; Woolard, D. L.; Samuels, A. C.; Gelmont, B. L.; Hesler, J. L.; Crowe, T. W.; Bykhovskaia, M. *J. Appl. Phys.* **2002**, *91*, 6106–6113.
(8) Globus, T. R.; Woolard, D.; Bykhovskaia, M.; Gelmont, B.; Werbos, L.; Samuels, A. C. *Int. J. High Speed Electron. Syst.* **2003**, *13*, 903–936.
(9) Sinden R. R. *DNA Structure and Function*; Academic Press: San Diego, CA, 1994.
(10) Heinemann, U.; Alings, C.; Bansal, M. *EMBO J.* **1992**, *11*, 1931–1939.
(11) Kypr, J.; Chládková, J.; Zimulová, M.; Vorlíčková, M. *Nucleic Acids Res.* **1999**, *27*, 3466–3473.
(12) Fasman, G. D. *Circular Dichroism and the Conformational Analysis of Biomolecules*; Plenum Press: New York, 1996.
(13) Gray, D. M.; Ratliff, R. L.; Vaughan, M. R. *Methods Enzymol.* **1992**, *211*, 389–406.
(14) Globus, T.; Bykhovskaia, M.; Woolard, D. L.; Gelmont, B. *J. Phys. D: Appl. Phys.* **2003**, *36*, 1314–1322.
(15) Globus, T.; Woolard, D.; Crowe, T. W.; Khromova, T.; Gelmont, B.; Hesler, J. *J. Phys. D: Appl. Phys.* **2006**, *39*, 3405–3413.
(16) Globus, T.; Khromova, T.; Woolard, D.; Gelmont, B. *Proc. SPIE* **2004**, *5268*, 10–18.
(17) Case, D. A.; Pearlman, D. A.; Caldwell, J. W.; Cheatham, T. E., III.; Wang, J.; Ross, W. S.; Simmerling, C. L.; Darden, T. A.; Merz, K. M.; Stanton, R. V.; Cheng, A. L.; Vincent, J. J.; Crowley, M.; Tsui, V.; Gohlke, H.; Radmer, R. J.; Duan, Y.; Pitera, J.; Massova, I.; Seibel, G. L.; Singh, U. C.; Weiner, P. K.; Kollman, P. A. AMBER 8; University of California: San Francisco, CA, 2004. http://ambermd.org/.
(18) Wang, J.; Cieplak, P.; Kollman, P. A. *J. Comput. Chem.* **2000**, *21*, 1049–1074.
(19) Li, X.; Bykhovski, A.; Gelmont, B.; Globus, T.; Woolard, D.; Bykhovskaia, M. *Proc. IEEE Conf. Nanotechnol., 5th* **2005**, 375–378.
(20) Teeter, M. M. *J. Phys. Chem.* **1990**, *94*, 8091–8097.
(21) Bykhovskaia, M.; Gelmont, B.; Globus, T.; Woolard, D. L.; Samuels, A. C.; Ha-Duong, T.; Zakrzewska, K. *Theor. Chem. Acc.* **2001**, *106*, 22–27.
(22) Beveridge, D. L.; Barreiro, G.; Byun, K. S.; Case, D. A.; Cheatham, T. E., III.; Dixit, S. B.; Giudice, E.; Lankas, F.; Lavery, R.; Maddocks, J. H.; Osman, R.; Seibert, E.; Sklenar, H.; Stoll, G.; Thayer, K. M.; Varnai, P.; Young, M. A. *Biophys. J.* **2004**, *87*, 3799–3813.
(23) Berendsen, H. J. C.; Postma, J. P. M.; van Gunsteren, W. F.; DiNola, A.; Haak, J. R. *J. Chem. Phys.* **1984**, *81*, 3684–3690.
(24) Essmann, U.; Perera, L.; Berkowitz, M. L.; Darden, T.; Lee, H.; Pedersen, L. G. *J. Chem. Phys.* **1995**, *103*, 8577–8593.
(25) Karplus, M.; Kushick, J. N. *Macromolecules* **1981**, *14*, 325–332.
(26) Levy, R. M.; Karplus, M.; Kushick, J.; Perahia, D. *Macromolecules* **1984**, *17*, 1370–1374.
(27) Vorlíčková, M.; Kypr, J.; Sklenář, V. Nucleic Acids: Spectroscopic Methods. In *Encyclopedia of Analytical Science*, 2nd ed.; Townshend, A., Poole, C. F., Eds.; Elsevier: Oxford, 2005; Vol. 6, pp 391−399.
(28) Hayward, S.; Kitao, A.; Go, N. *Proteins: Struct., Funct., Genet.* **1995**, *23*, 177–186.
(29) Woods, K. N.; Lee, S. A.; Holman, H.-Y. N.; Wiedemann, H. *J. Chem. Phys.* **2006**, *124*, 224706–8.

JP806630W